

SPECTRAL PROPERTIES OF A TERAHERTZ OSCILLATOR BASED ON THE $\text{Bi}_2\text{Sr}_2\text{CaCu}_2\text{O}_{8+\delta}$ MESASTRUCTURE

N. V. Kinev,^{1*} L. V. Filippenko,¹ M. Y. Li,² J. Yuan,²
H. B. Wang,² and V. P. Koshelets¹

UDC 621.382.2

Experimental results of the study of the radiation spectra of an oscillator based on the mesastucture of a high-temperature superconducting $\text{Bi}_2\text{Sr}_2\text{CaCu}_2\text{O}_{8+\delta}$ crystal are presented. The oscillator operating modes are studied, the terahertz radiation in the range 450–750 GHz is obtained, and the Lorentzian shape of the spectral line is measured. It is shown that the minimum oscillation linewidth amounts to 65 MHz. The possibility of phase stabilization of the oscillator radiation is demonstrated.

1. INTRODUCTION

In recent two decades, increased attention has been devoted to tunable terahertz oscillators, which are mostly required in astrophysics and radio astronomy [1, 2], and are also of interest to medical diagnostics [3–5] and safety systems [5, 6].

The complexity of developing such devices is stipulated by the so-called terahertz gap, i.e., a sufficiently wide frequency range in which the physical processes effectively operating in both lower-frequency radio range and the higher-frequency infrared range become low-efficient or totally inefficient. Moreover, the requirements to terahertz-range oscillators are constantly increasing with the science and technology development. Among the basic requirements are the high signal stability, a sufficient power for solving various problems, and the presence of certain spectral properties, which ensure the frequency resolution of superheterodyne receivers when the terahertz source is used as a local oscillator.

The devices based on high-temperature superconducting cuprates [7–9] are the most promising ones among the recently proposed oscillators. The main advantages of such oscillators are related to their compactness, small weight and size (compared with, e.g., backward-wave oscillators or laboratory gas lasers), which is mostly important for the space and radio astronomy applications, and relatively low cost and manufacturing simplicity. In addition, such oscillators can be integrated in a single device with a mixer in the feedback circuit to realize phase stabilization of the signal [10]. Such a composite device can operate as both a powerful high-stability local oscillator for the terahertz receivers and new-generation spectrometers which are capable of covering the major part of the terahertz gap.

A $\text{Bi}_2\text{Sr}_2\text{CaCu}_2\text{O}_{8+\delta}$ (BSCCO) crystal is the most promising example of such materials that are used as the basis for developing oscillators. Despite the fact that the Josephson structure inside such a material at the crystalline level was discovered over 20 years ago [11], the intense studies of the corresponding oscillators have started only recently in [12] in which a comparatively powerful electromagnetic emission of this crystal in the terahertz frequency range has experimentally been observed. Over 2000 papers, both experimental [13–16] and theoretical [17–19], have been published in recent five years in the leading scientific journals

* nickolay@hitech.cplire.ru

¹ V. A. Kotel'nikov Institute of Radio Engineering and Electronics of the Russian Academy of Sciences, Moscow, Russia ² Nanking University, Nanking, China. Translated from *Izvestiya Vysshikh Uchebnykh Zavedenii, Radiofizika*, Vol. 56, Nos. 8–9, pp. 647–656, August–September 2013. Original article submitted May 15, 2013; accepted September 30, 2013.

on the development and study of such oscillators. Despite great interest evoked among many research groups worldwide in this direction of cryogenic electronics, only recently we have measured the spectral characteristics of a BSCCO oscillator with accuracy exceeding its autonomous oscillation linewidth [20]. Previously, all the known spectral measurements of such structures were performed using the Fourier spectrometers with resolution worse than 1 GHz (see, e.g., [21]).

In this work, we present the results of the pioneer studies of the spectral characteristics of the oscillators based on BSCCO monocrystal mesastructures, which were conducted by the researchers of V. A. Kotel'nikov Institute of Radio Engineering and Electronics of the Russian Academy of Sciences (Moscow, Russia) in cooperation with the colleagues from Nanking University (Nanking, China). The samples of oscillators were manufactured using the processing equipment of National Institute for Materials Science (Tsukuba, Japan). The oscillator design and the experimental facility for its study are described in Sec. 2. In Sec. 3, the current-voltage characteristics and operating modes of the oscillator are described. The results of studying operation of the oscillator at the terahertz frequencies and its spectral characteristics are presented in Sec. 4. The possibilities of stabilization of the oscillator frequency and power using the phase-locked loop are discussed in Sec. 5. Our conclusions are presented in Sec. 6.

2. OSCILLATOR AND EXPERIMENTAL-FACILITY DESIGN

The oscillator on the basis of high-temperature $\text{Bi}_2\text{Sr}_2\text{CaCu}_2\text{O}_{8+\delta}$ cuprate is a monocrystal structure in the form of a mesa (layered structure) obtained using the crystal etching by the focused argon ion beam [15]. A system of the series-connected Josephson junctions exists in such a material on the crystalline level. In such structures, the superconductivity is stipulated by the pair layers (bilayers) of CuO_2 with a thickness of about 0.3 nm. These bilayers are separated by the SrO and Bi_2O_3 layers working as barriers, which naturally forms the cells in the form of Josephson structures in the crystalline lattice [7, 22]. The cell thickness (i.e., the lattice constant) is 1.533 nm. Therefore, the crystal with such a structure having the shape of a mesa with a thickness of about 1.5 μm has an array of $N \approx 1000$ series-connected identical Josephson junctions. If voltage of the order of 1 V is applied to such a structure (in this case, the voltage at each junction is about 1.0–1.5 mV), an electromagnetic signal in the terahertz frequency range is observed at the output. Today, its power level attains tens of microwatts [23]. Typical mesastructure length and width are of the order of 100–400 μm and 30–100 μm , respectively.

The studied BSCCO based oscillator and the circuits for its connection to the bias and measurement units are shown in Fig. 1. Its operation was studied in the regime where the bias current across the structure was specified. To maximally reduce external fluctuations in the current-specification and voltage-measurement system, we used a battery unit with low-level natural noise. This allows us to avoid low-frequency technical noise, for example, power-supply noise with a frequency of 50 Hz. To specify and monitor the oscillator temperature, the sample holder was equipped with a heater and a temperature detector. Therefore, the system was capable of adjusting the temperature in a sufficiently wide range from 4.5 K (liquid helium temperature) to a value of the order of 100 K. In this case, the critical temperature T_c of transition of the high-temperature superconductor to normal state is about 95 K.

The spectral characteristics of the oscillator were studied using the high-sensitivity superheterodyne superconducting integral receiver on the basis of a quasi-particle nonlinearity of the superconductor–insulator–superconductor (SIS) junction operating as a mixer, which was developed at V. A. Kotel'nikov Institute of Radio Engineering and Electronics of the Russian Academy of Sciences [24–26]. Such a receiver

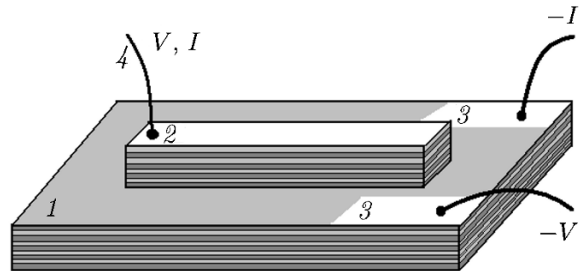


Fig. 1. Layout of an oscillator based on the high-temperature superconducting mesastructure: $\text{Bi}_2\text{Sr}_2\text{CaCu}_2\text{O}_{8+\delta}$ monocrystal (1), $330 \times 50 \mu\text{m}$ mesa (2), gold contact platforms (3), and wires to ensure connection with the measuring circuit (4).

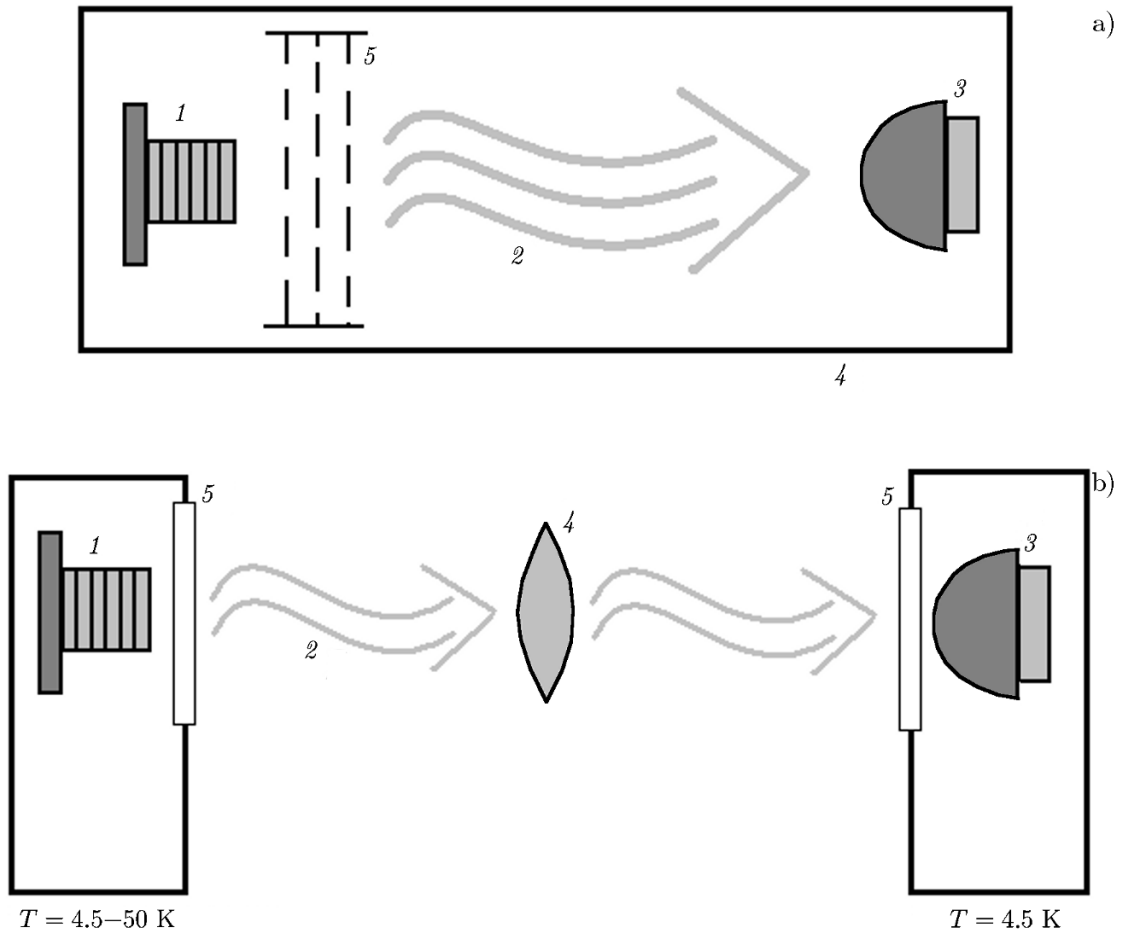


Fig. 2. Setups for studying the spectral characteristics of the oscillator on the basis of $\text{Bi}_2\text{Sr}_2\text{CaCu}_2\text{O}_{8+\delta}$ crystals. Oscillator 1 emits terahertz signal 2, which is recorded by superconducting integral receiver 3 installed on the lens. Panel a shows the oscillator and the receiver located in a single cryostat inside magnetic screen 4 so that several (one to three) “Gortex” thermal infrared filters 5 are mounted between the devices. The oscillator and receiver locations in different cryostats are shown in panel b, where focusing lens 4 is used to narrow the directional pattern, and windows 5 are mounted on the cryostats.

is intended to perform spectral studies of the electromagnetic radiation in the frequency range 450–700 GHz and successfully used for measuring the profiles of the spectral lines of the gas-molecule radiation and absorption and for the spectral study of any external terahertz oscillator radiating in the operation frequency range of the receiver. The best noise temperature of the superheterodyne superconducting integral receiver is 120 K and its spectral resolution is better than 0.1 MHz, which exceeds the resolution of modern terahertz-range Fourier spectrometers by several orders of magnitude.

Two layouts of the oscillator and receiver location with respect to each other were tested in this work. In the first case, the oscillator was located in a cryostat of the superheterodyne superconducting integral receiver in the immediate vicinity of the mixing unit of the receiver (Fig. 2a). In the second case, the oscillator and the receiver were located in independent cryostats and radiation from one cryogen facility to the other was directed through Mylar quasioptical windows (Fig. 2b). The integral receiver is operated at a temperature of about 4.5 K, whereas the optimal BSCCO-oscillator temperature is 40–50 K. The location of the devices close to each other leads to overheating and substantially deteriorates the operating characteristics of the local oscillator, which makes operation of the superheterodyne superconducting integral receiver impossible in its usual operating frequency band even despite the presence of several thermal “Gortex” screens. Therefore, the most successful studies were conducted when the devices were located in independent

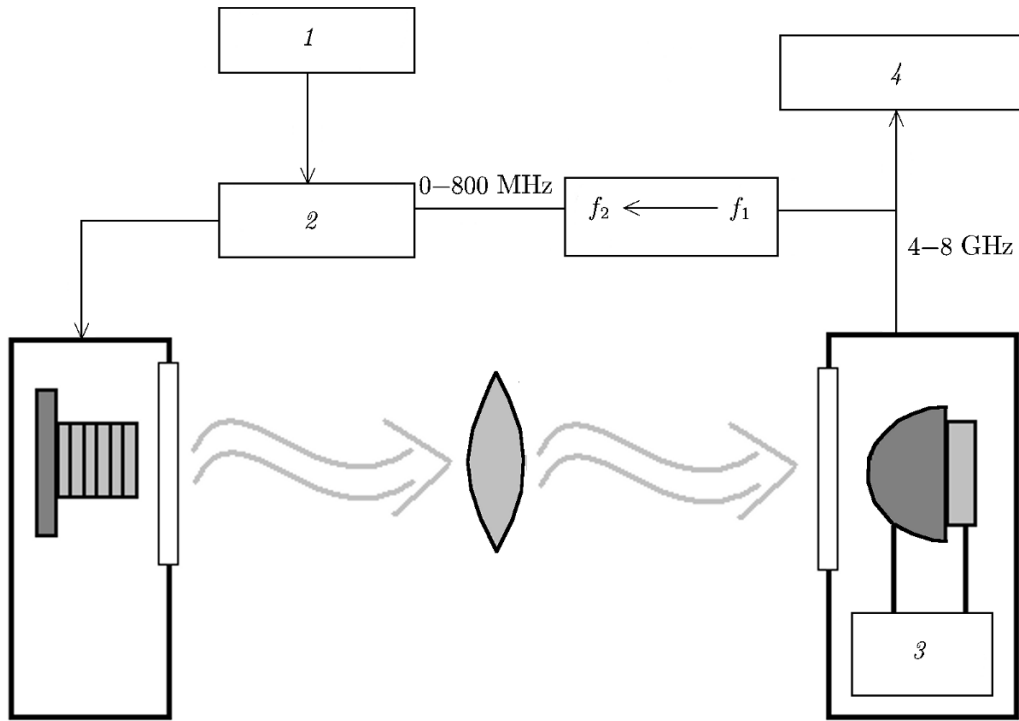


Fig. 3. Setup of the experimental facility using synchronization of the BSCCO-oscillator by the reference signal with a frequency of 400 MHz with the help of the noncooled phase-locked loop. The local oscillator of the integral receiver was synchronized using an independent phase-locked loop with a reference signal at a frequency of 400 MHz; reference signal at a frequency of 400 MHz (1), noncooled phase-locked loop (2), independent phase-locked loop (3), and spectrum analyzer (4).

cryostats. The spectral lines of the oscillator radiation are recorded using the superheterodyne superconducting integral receiver and displayed on the spectrum-analyzer screen in the intermediate-frequency range 4–8 GHz. The spectrum analyzer allows one to average the signal, read it by a computer, and perform other necessary digital operations for the spectrum analysis and processing.

The noncooled phase-locked loop the signal to which was sent from the SIS mixer of the integral receiver was used for the frequency and phase stabilization of the oscillator. In this case, the reference-signal frequency was 400 MHz, while the local oscillator of the receiver was stabilized using an independent phase-locked loop. The output signal of the SIS mixer in the intermediate-frequency range 4–8 GHz was transferred to the range 0–800 MHz using the frequency converter and the reference signal at the frequency 3.6 GHz. The diagram of this facility is shown in Fig. 3. Therefore, the SIS mixer not only recorded the radiation spectrum of the BSCCO oscillator, but also was an element in the feedback circuit for its stabilization.

3. CURRENT-VOLTAGE CHARACTERISTICS AND OPERATING MODES OF THE OSCILLATOR

The current-voltage characteristics of the oscillator at various temperatures are shown in Fig. 4. The jump to the current-voltage characteristic branch, corresponding to the resistive state occurred for bias currents of about 25 mA. In this case, the shape of the characteristic had hysteresis typical of the tunnel junctions. The current-voltage characteristic has a part with negative differential resistance, which is caused by the sample heating and variation in not only the gap voltage at the junctions, but also the number of junctions in the superconducting state due to the appearance of the so-called “hot spot” region [21]. It should also be noted that Fig. 4 shows a general view of the current-voltage characteristic of such an oscillator

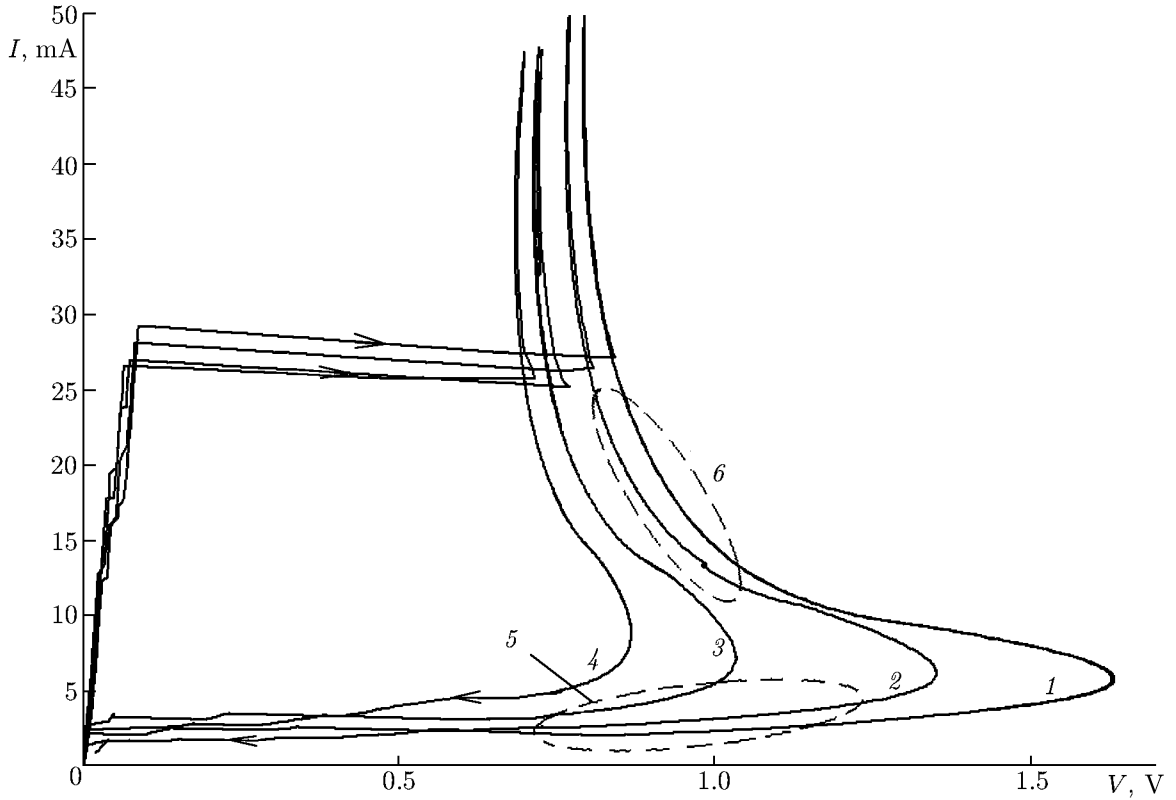


Fig. 4. Oscillator current-voltage characteristics measured at different temperatures: curve 1 corresponds to $T = 4.5$ K, curve 2, to 17 K, curve 3, to 32 K, curve 4, to 42 K, curve 5, to the low-current mode, and curve 6, to the high-current mode. The arrows show the current-variation direction along the curves. The dashed contours denote the oscillator operating modes.

for the wide-range current variation. In fact, the full pattern is more complicated since the operating-point location can depend on the path of transition to the given point (in the plane of the current intensity I and the voltage V). Such a feature of the current-voltage characteristic is due to the system consisting of a large number of junctions which are in the superconducting state at various segments of the characteristic and, therefore, contribute to the total mesostructure voltage.

The radiated-power measurement demonstrates two operating modes of the BSCCO oscillator [13, 21], namely, for the current values above (high-current mode) and below (low-current mode) the point of the voltage maximum. The radiation in the low-current mode was discovered for the first time. Therefore, it was assumed that in this mode, the spectral characteristics for the branch of the current-voltage characteristic with positive differential resistance R_d are better than those on the branch with negative R_d . We showed for the first time [20] that this assumption is erroneous and the oscillator has much better spectral characteristics in the high-current mode. This issue is discussed in detail in the next section.

4. OSCILLATOR SPECTRAL CHARACTERISTICS

The distinctive feature of determining the oscillator frequency f_n (compared with a single Josephson emitter) is that the mesostructure bias voltage is divided among N junctions:

$$f_n = \frac{2e}{h} V_n = \frac{2e}{h} \frac{V_{\text{bias}}}{N}, \quad N \neq \text{const}, \quad (1)$$

where V_n is the voltage on one junction in the array, V_{bias} is the total voltage on the mesostructure, e is the elementary charge, and h is Planck's constant. The left-hand side of Eq. (1) is merely the Josephson

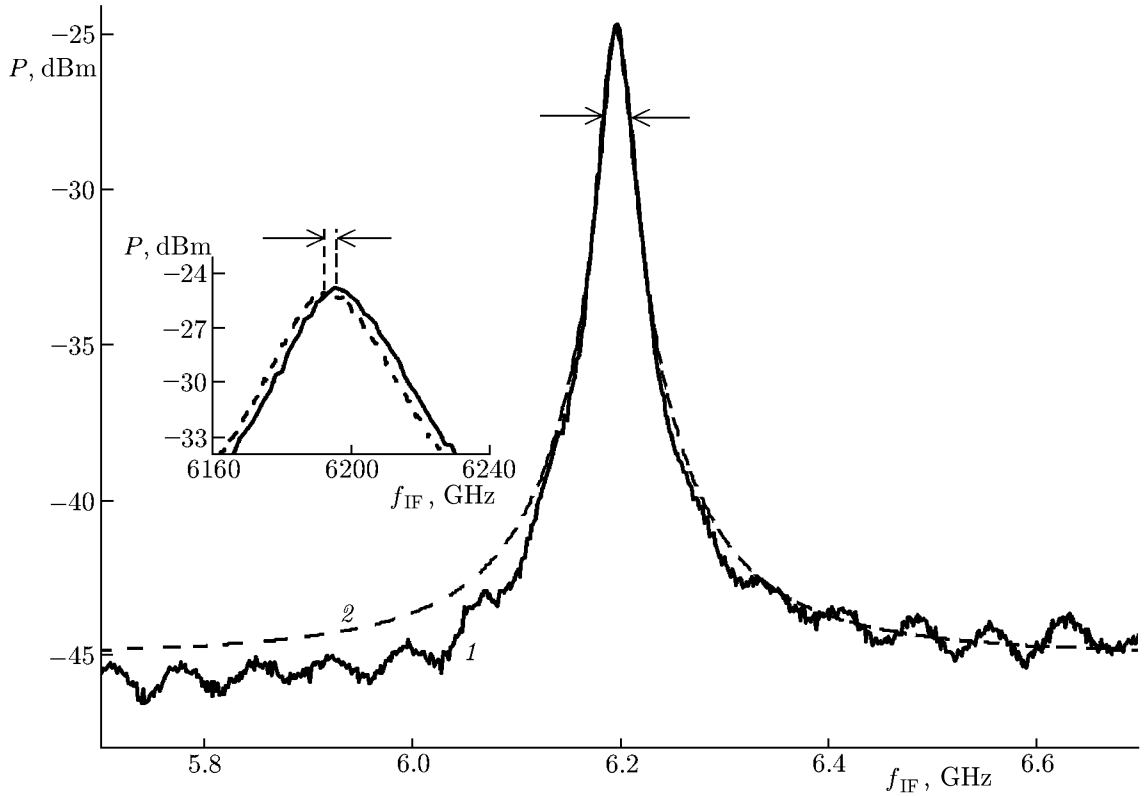


Fig. 5. Oscillator radiation spectrum measured using a superheterodyne superconducting integral receiver with the intermediate-frequency range 4–8 GHz (1) and a Lorentzian-shape curve (2). The frequency $f_0 = 611.95$ GHz, the operation temperature is 44 K, the number of junctions $N \approx 570$, and the linewidth is 23 MHz. The measurements were conducted in the high-current mode. The left-hand inset shows the shift of the radiation-line peak due to a free drift of the system by 3 MHz in 3 min, P is the power, and f_{IF} is the intermediate frequency.

relationship. In this case, the oscillator frequency f_n can be determined experimentally with high accuracy if the spectral characteristics are measured by the superheterodyne superconducting integral receiver and the following formula is used:

$$f_n = f_{LJJ} \pm f_{IF}^{SIS}, \quad (2)$$

where frequency f_{IF}^{SIS} is determined by the oscillation-line location on the spectrum-analyzer screen and lies in the output-signal range 4–8 GHz of intermediate frequencies of the SIS mixer, and the sign on the right-hand side of Eq. (2) depends on which intermediate-frequency band (shifted upwards or downwards with respect to the local-oscillator frequency) is measured. In the case where the oscillator frequency f_n is known, Eq. (1) can be used for calculating the number N of the junctions participating in the Josephson oscillation.

Figure 5 shows the characteristic spectrum of the oscillator radiation (curve 1) at the frequency $f_0 = 611.95$ GHz, which was measured at the temperature $T = 44$ K in the high-current mode. The number of the junctions used in oscillation amounts to $N \approx 570$. The linewidth was 23 MHz, while the line shape is Lorentzian with a high degree of accuracy (curve 2). The left-hand inset in Fig. 5 indicates high stability of the oscillation line, i.e., the line shift was only 3 MHz during the waiting time equal to 3 min because of the system drift, i.e., the shift value is an order of magnitude smaller than the linewidth.

Figure 6 shows the result of the radiation-linewidth measurement for different temperatures and operating modes. In this case, the realized frequency range was from 450 to about 750 GHz. It should be noted that the upper boundary of this range (i.e., maximum measured frequency $f_{max} = 736$ GHz) is

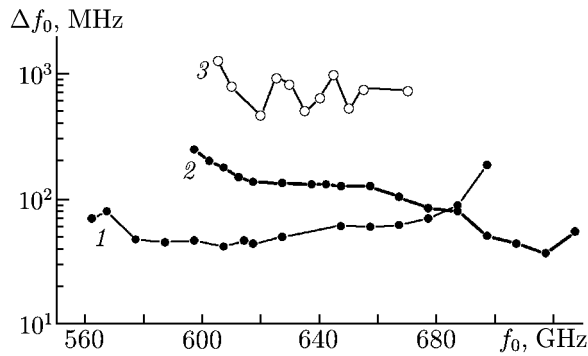


Fig. 6. Oscillator-radiation linewidth Δf_0 as a function of the frequency f_0 for different temperatures and operating modes at the current-voltage characteristic. Curve 1 corresponds to $T = 40$ K and the high-current mode, curve 2, to $T = 32$ K and the low-current mode and curve 3, to $T = 35$ K and the low-current mode.

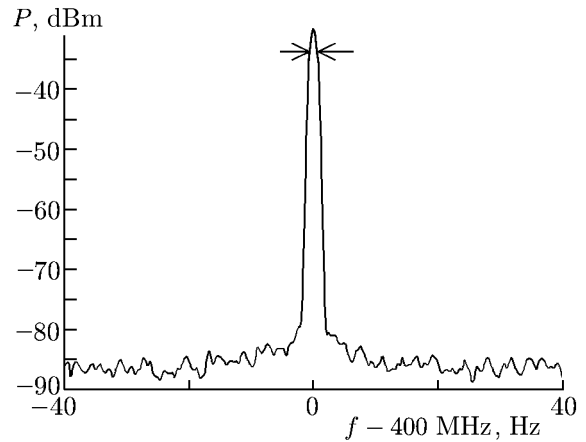


Fig. 7. Oscillator spectral characteristics measured in the regime of phase lock to the reference signal at a frequency of 400 MHz for the radiation frequency $f_0 = 557$ GHz, the operation temperature about 35 K, and the spectrum-analyzer resolution 1 Hz. The linewidth was of the order of 1 Hz when the stabilization system with the phase-locked loop was used.

determined by the properties of the superheterodyne superconducting integral receiver whose local oscillator operates up to a frequency of about 750 GHz, whereas the BSCCO-oscillator power is higher at the higher frequencies [23]. Experiments with the series of the BSCCO-oscillator samples under different temperature regimes showed a still narrower radiation line with a width of up to 6 MHz. To reach the maximum possible frequency-tuning width of a superheterodyne superconducting integral receiver, the devices were located in different cryostats (Fig. 2b) for avoiding mutual thermal influence of the oscillator and the receiver. The majority of the results were obtained exactly for this configuration of the system.

It is very important that the highest-quality spectral characteristics (the linewidth 6–50 MHz) were recorded only in the high-current mode. On the contrary, the low-current mode shows sufficiently wide oscillation lines exceeding 500 MHz (see curve 3 in Fig. 6). This is probably related to the fact that a certain radiation-synchronization mechanism whose nature has not yet been completely studied is absent for a small current. We believe that the presence of the “hot spot” [13, 19], which appears only for a high bias current, or the presence of a sufficiently high-quality resonator, which is electrodynamically coupled to the BSCCO oscillator, can be the synchronization condition in the conducted measurement series. Thus, it was shown that the high-current mode is the only possible operating mode of the high-temperature superconducting mesastructure as a terahertz oscillator.

5. PHASE LOCK OF THE RADIATION FREQUENCY

Signal stability is one of the main applicability factors of any oscillator for solving a particular practical problem. In this work, we performed a series of experiments on the oscillator stabilization using an additional uncooled phase-locked loop. The experimental setup is shown in Fig. 3. Intermediate-frequency signal of the integral receiver whose local oscillator operated in the phase-lock regime was used for the synchronization. Under certain oscillator-operation conditions such as temperature, frequency, and operating point on the current-voltage characteristic, the oscillator phase-lock loop was effectively realized. The result of the reference-signal synchronization is shown in Fig. 7. The measurement was performed using the spectrum analyzer with a maximum frequency resolution of 1 Hz. For the given autonomous linewidth (about 20 MHz), the relative spectral power at the central peak was about 10%. Therefore, we demonstrated the possibility

to stabilize the BSCCO oscillator in principle on the basis of a large Josephson-junction array realized in the form of a monocrystal mesastructure. The possibility of oscillator-frequency synchronization over the entire operating range needs a comprehensive study of the oscillation mechanisms in such structures. Until now, the mechanisms of internal synchronization of the Josephson-junction system, as well as the factors determining the spectral characteristics of the oscillator, i.e., radiation linewidth and power have not yet been definitely revealed. Therefore, a complex and adequate theory, which describes the physical mechanisms in the high-temperature superconducting BSCCO oscillators, should be developed.

6. CONCLUSIONS

This work is aimed at studying the terahertz oscillator on the basis of a high-temperature superconducting $\text{Bi}_2\text{Sr}_2\text{CaCu}_2\text{O}_{8+\delta}$ mesastructure, which is an array of $N \approx 1000$ series-connected Josephson junctions formed by the natural crystal structure. The spectral characteristics of such an oscillator were studied with an accuracy that exceeds the autonomous linewidth of its oscillation by many times. The oscillation frequency band 450–750 GHz and the Lorentzian shape of the spectral line with a width of 6 to over 750 MHz are realized and high signal stability is demonstrated. It is shown that the regime of high bias currents is the only possible operating mode of such an oscillator as a local oscillator, while the low-current mode can be used for creating a source of wideband terahertz noise with bandwidth from fractions of to several gigahertz. The possibility to perform phase stabilization of the BSCCO-oscillator radiation is demonstrated in principle. Frequency stabilization over the entire operating range is now the most topical and promising task in the development and study of such devices.

The conducted studies are an important step towards the practical use of BSCCO oscillators and the creation of complex devices on their basis. In particular, the development of an integral structure combining the BSCCO oscillator and the harmonic SIS mixer used in the feedback loop with the oscillator for its synchronization is a promising direction of the corresponding studies. Such a device can work as a high-power high-stability terahertz oscillator and will find application for atmospheric monitoring, radio astronomy, and other science and technology fields, e.g., medicine and safety systems.

REFERENCES

1. K. Suto and J. Nishizawa, *Int. J. Infrared Millimeter Waves*, **26**, No. 7, 937 (2005).
2. J. W. Kooi, “*Advanced receivers for submillimeter and far infrared astronomy, PhD thesis*”, Print Partners Ipskamp B.V., Enschede (2008).
3. B. M. Fischer, M. Walther, and P. U. Jepsen, *Phys. Medicine Biology*, **47**, No. 21, 3807 (2002).
4. K. Humphreys, J. P. Loughran, M. Gradziel, et al., in: *Proc. 26th Ann. Int. Conf. IEEE EMBS, San Francisco, CA, USA* (2004), vol. 1, p. 1302.
5. D. Gerecht, Gu D. S. Yngvesson, et al., in: *Joint 30th Int. Conf. Infrar. Millim. Waves* (2005), vol. 1, p. 9.
6. J. F. Federici, B. Schulkin, F. Huang, et al., *Sci. Technol.*, **20**, 266 (2005).
7. K. M. Shen and J. C. Seamus Davis, *Materials Today*, **11**, No. 9, 14 (2008).
8. http://en.wikipedia.org/wiki/High-temperature_superconductivity#Cuprates.
9. L. N. Bulaevskii and A. E. Koshelev, *Phys. Rev. Lett.*, **99**, No. 5, 057002 (2007).
10. D. Y. An, J. Yuan, N. Kinev, et al., *Appl. Phys. Lett.*, **102**, No. 9, 092601 (2013).
11. R. Kleiner, F. Steinmeyer, G. Kunkel, et al., *Phys. Rev. Lett.*, **68**, No. 15, 2394 (1992).
12. L. Ozyuzer, A. E. Koshelev, C. Kurter, et al., *Science*, **318**, 1291 (2007).
13. H. B. Wang, S. Guenon, J. Yuan, et al., *Phys. Rev. Lett.*, **102**, No. 1, 017006 (2009).

14. H. Minami, I. Kakeya, H. Yamaguchi, et al., *Appl. Phys. Lett.*, **95**, No. 23, 232511 (2009).
15. S. Guenon, M. Grunzweig, B. Gross, et al., *Phys. Rev. B*, **82**, No. 21, 214506 (2010).
16. M. Tsujimoto, T. Yamamoto, K. Delfanazari, et al., *Phys. Rev. Lett.*, **108**, No. 10, 107006 (2012).
17. S. Lin and X. Hu, *Phys. Rev. Lett.*, **100**, No. 24, 247006 (2008).
18. V. M. Krasnov, *Phys. Rev. Lett.*, **103**, No. 22, 227002 (2009).
19. A. Yurgens, *Phys. Rev. B*, **83**, No. 18, 184501 (2011).
20. M. Y. Li, J. Yuan, N. Kinev, et al., *Phys. Rev. B*, **86**, No. 6, 060505 (2012).
21. H. B. Wang, S. Guenon, B. Gross, et al., *Phys. Rev. Lett.*, **105**, No. 5, 057002 (2010).
22. R. Kleiner, *Science*, **318**, 1254 (2007).
23. T. Kashiwagi, M. Tsujimoto, T. Yamamoto, et al., *Jpn. J. Appl. Phys.*, **51**, No. 1, 010113 (2012).
24. V. P. Koshelets and S. Shitov, *Supercond. Sci. Technol.*, **13**, R53 (2000).
25. V. P. Koshelets, P. N. Dmitriev, A. B. Ermakov, et al., *Radiophys. Quantum Electron.*, **48**, Nos. 10–11, 844 (2005).
26. V. P. Koshelets, A. B. Ermakov, L. V. Filippenko, et al., *Proc. SPIE*, **7854**, No. 78540J (2010).